Magnetic, thermodynamic and optical properties of Sb-substituted Ba_2PrBiO_6 double perovskite oxides

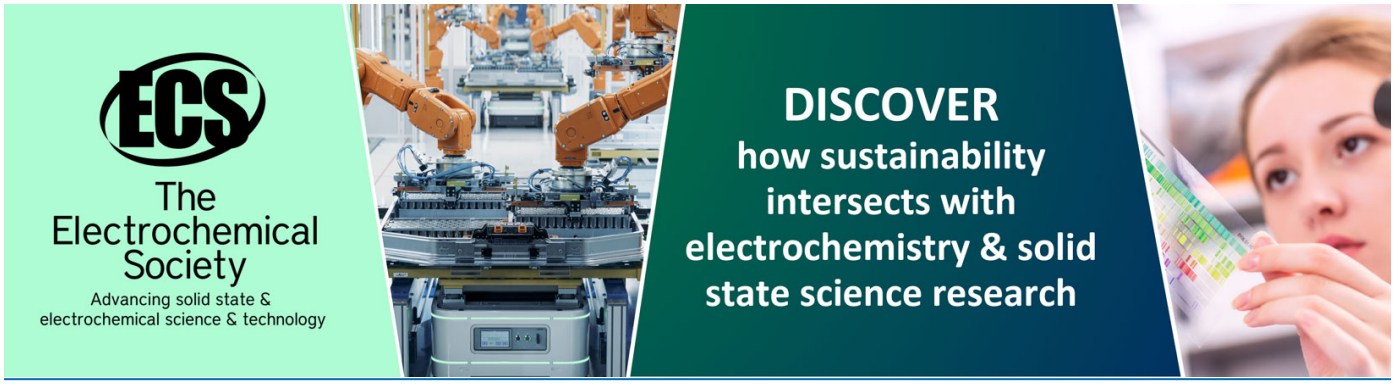

IOP Conf. Series: Journal of Physics: Conf. Series **969** (2018) 012122 doi:10.1088/1742-6596/969/1/012122

Magnetic, thermodynamic and optical properties of Sb-substituted Ba_2PrBiO_6 double perovskite oxides

K. Onodera, T. Kogawa, M. Matsukawa, H. Taniguchi, K. Nishidate
Faculty of Science and Engineering, Iwate University, Morioka 020-8551, Japan
E-mail: matsukawa@iwate-u.ac.jp

A. Matsushita, M. Shimoda
National Institute for Materials Science, Tsukuba, Ibaraki 305-0047, Japan

Abstract. We demonstrated crystal structures, magnetic, thermodynamic and optical properties of the B-site substituted perovskite oxides $Ba_2Pr(Bi_{1-x},Sb_x)$ O_6 (x=0, 0.1 and 0.2). Polycrystalline samples of Sb-substituted Ba_2PrBiO_6 were prepared with the conventional solid-state reaction technique. The X-ray diffraction data revealed that the polycrystalline samples are an almost single phase with a monoclinic structure ($C2/m$). Substitution of smaller Sb ion at Bi site causes a monotonic decrease in both the lattice parameters and volume. Magnetization measurements at high temperatures above 200 K show that the effective magnetic moment is estimated to be around 3.15 μ_B, which is close to that for Pr^{3+}ion. The X-ray photoemission spectroscopy analysis revealed that a prominent peak of Pr^{3+} is dominant with a smaller shoulder structure of Pr^{4+}. A Schottky-like anomaly observed in the low-temperature specific heat measurement is explained by low-lying splitting of Pr ions under the crystal field effect. Optical spectra were measured using a diffuse-reflectance method. The band gaps were estimated from the optical data to be 0.977 eV and 1.073 eV, at x=0 and 0.2, respectively. The effect of band gap opening due to Sb substitution is examined by using the density functional theory.

1. Introduction

A large number of double perovskite oxides $A_2B'B''O_6$ have been widely studied due to their attractive physical properties and potential applications[1, 2]. Some of semiconducting $A_2B'B''O_6$ compounds exhibit photocatalytic properties such as hydrogen generation by water splitting and are taken as alternative materials for TiO_2 oxide [3]. In particular, Ba_2PrBiO_6 compound has been shown to possess high photocatalytic activity, which is probably related to the valence mixing[4, 5]. A previous study on the magnetic states of Ba_2PrBiO_6 compound suggests an anomalous valence situation for Pr ions.[6] The complicated ground states of rare earth ions such as Pr ion under the crystal field effect remain open question, not only in the physical properties of the double perovskite compound, but also in the view point of physics of $4f$ electron systems.

There are significant factors such as charge and size differences between B' and B'' sites, to determine the B-site ordering of the double perovskite oxide[7]. Increase in lattice strain and/or increase in the electrostatic repulsion overcome the entropy contribution toward disordering, causing the alternate arrangement. For $A_2^{2+}B'^{3+}B''^{5+}O_6$ composition, the B sites tend to oder

with increasing the ion size difference $\triangle r_B = r_{B'} - r_{B''}$. If $\triangle r_B > 0.2$ Å, it is well known that the B sites of the compounds are almost ordered alternately in the all crystallographic axes[7]. In $Ba_2^{2+}Pr^{3+}Bi^{5+}O_6$ compound, the B-site ionic radius difference $\triangle r_B = 0.23$ Å meets the above condition, suggesting the B-site ordering. ($r_{B'}$ (Pr^{3+})=0.99 Å and $r_{B''}$ (Bi^{5+})=0.76 Å.[8]) The density functional theory based calculation reveals the band structure and its associated orbital states of this compound, and predicts the stability of crystal structures of B site ordered states.

In this paper, we investigate crystal structures, magnetic, thermodynamic and optical properties of the $Ba_2Pr(Bi_{1-x},Sb_x)$ O_6 compounds (x=0, 0.1 and 0.2), to determine the physical properties of B-site substituted double perovskite oxide. For comparison, the physical properties of the B′site substituted Ba_2LaBiO_6 compound without magnetic ions are examined.

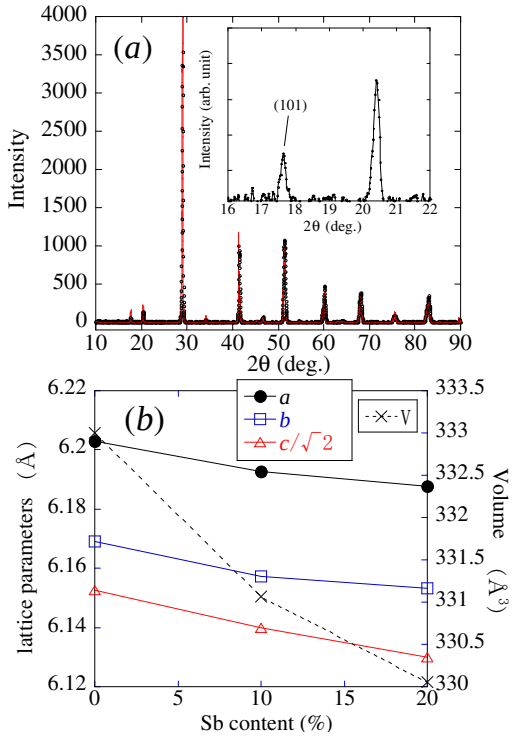

Figure 1. (a)X-ray diffraction patterns of the parent Ba_2PrBiO_6 compound. The (101) peak in the inset corresponds to one of typical Miller indexes of B-site ordered double-perovskite structure. The calculated curve was obtained by using the lattice parameters. (b)The lattice parameters and volume as a function of Sb content.

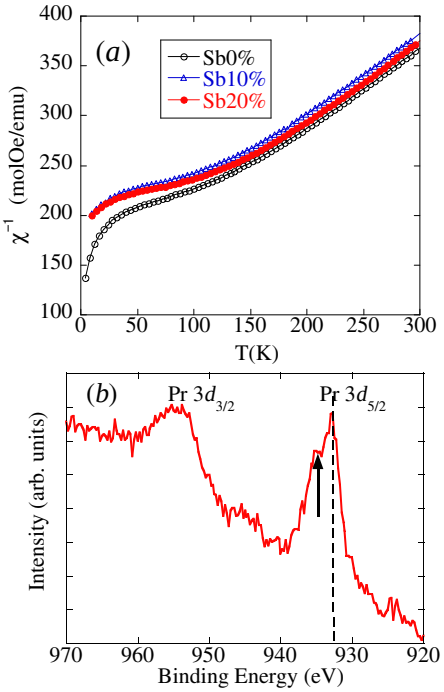

Figure 2. (a)Inverse magnetic susceptibilities (χ^{-1}) for $Ba_2Pr(Bi_{1-x},Sb_x)O_6$ (x=0, 0.1 and 0.2). (b)the XPS spectrum of Pr 3d core level emission for the parent sample. The dashed line corresponds to a peak position in the Pr^{3+} standard Pr_2O_3 spectrum. The arrow represents the Pr^{4+} standard peak position.

2. Experiment

Polycrystalline samples of Sb-substituted Ba_2PrBiO_6 were prepared with the conventional solid-state reaction technique. Stoichiometric mixtures of $BaCO_3$, Pr_6O_{11}, Bi_2O_3, and Sb_2O_3 powders were ground, sintered in air at 800-900 °C for 2 days with intermediate grindings, and pressed into pellets. The pellet samples were annealed in air at 1000 °C for 4 days. The X-ray diffraction data revealed that the polycrystalline samples are an almost single phase with a monoclinic structure

($C2/m$). For the parent Ba_2PrBiO_6, the lattice parameters are a = 6.2038Å, b = 6.1689Å, c = 8.7011Åand β = 89.7303°, which are in fair agreement with those reported by a previous study[6]. The emergence of (101) reflection indicates B-cation ordering which is characteristic of B-site ordered double-perovskite structure. Substitution of smaller Sb^{5+} (0.60 Å) ion at Bi^{5+} (0.76 Å) site causes a monotonic decrease in both the lattice parameters and volume as shown in Fig.1 (b). The *dc* magnetization was conducted at a magnetic field of 1 T under the zero-field cooling process using a superconducting quantum interference device magnetometer (MPMS,Quantum Design). X-ray photoemission spectroscopy (XPS) measurements for Pr 3d core-level emission were performed in a VG ESCALAB MkII spectrometer by using MgKα X-ray irradiation (1254 eV). Specific heat measurements were conducted by a thermal relaxation method using a physical property measuring system (PPMS,Quantum Design). Optical spectra were measured by using a diffuse-reflectance method with a spectrophotometer (Hitachi U-3500) and $BaSO_4$ was used as the reference material. Optical band gaps for the powder samples were evaluated from reflectance spectral data using the conventional Kubelka-Munk functions[6, 9] . We calculated the band structure of Ba_2PrBiO_6 by using the density functional theory as implemented in the code VASP.

3. Results and Discussion

The inverse magnetic susceptibilities (χ^{-1})for $Ba_2Pr(Bi_{1-x},Sb_x)O_6$ (x=0, 0.1 and 0.2) are shown in Fig.2(a) as a function of temperature at a magnetic field of 1 T. In the Ba_2LaBiO_6 compound, no magnetization signal was observed because of the absence of magnetic ions. From the magnetization data at high temperatures above 200 K, we estimate the effective magnetic moment according to the Curie-Weiss law. The value of effective magnetic moment μ_{eff} is evaluated by using the following formula,

$$C = N\mu_{eff}^2\mu_B^2/3k_B$$

where C, N, and μ_B denote the Curie constant, the number of magnetic atom per mol, and the Bohr magneton, respectively. Performing the calculation, we obtained that μ_{eff} = 3.15 μ_B and 3.12 μ_B for the parent and Sb20% samples, respectively. These values are close to the effective magnetic moment for the Pr^{3+} free ion (3.57μ_B). However, these findings do not exclude the presence of Pr^{4+}[5]. The XPS spectrum of Pr 3d core level for the parent sample is shown as a function of the binding energy in Fig 2 (b). The XPS profile strongly suggests that a prominent peak of Pr^{3+} is dominant at the specified binding energy values around 933 eV, followed by a smaller shoulder structure of Pr^{4+} around 935 eV. The dashed line corresponds to a peak position in the Pr^{3+} standard Pr_2O_3 spectrum. The arrow points to the Pr^{4+} standard PrO_2 spectrum.

In Fig. 3(a), specific heats of the parent Ba_2PrBiO_6 and its related Ba_2LaBiO_6 compounds are shown as a function of temperature between 2 and 300 K. In addition, we plot in Fig. 3(b) low-temperature specific heat data of both the samples, C/T(Pr) and C/T(La). Applying the Debye T^3 law to the low temperature data, we estimate the Debye temperature, θ=112 K for Ba_2LaBiO_6. We assume that the lattice component in C/T of the parent sample is almost equivalent to the values of C/T of the nonmagnetic Ba_2LaBiO_6 compound since both samples share the same crystal structure. Thus, specific heat differences dC/T between both compounds are taken as non lattice components of the parent sample. A Schottky-type specific heat with two energy levels [10] is given by

$$C_{\mathrm{Sch}} = k_B(x/2)^2/\cosh^2(x/2) \text{ with } x = \triangle E/k_BT.$$

When the crystal field splitting between the ground and low-lying excited states of this compound is set to be $\triangle E$ =1.5 meV, we obtain a good agreement between the calculated curve and

experimental data. Accordingly, we attribute the observed broad peak in C/T to the Schottky-type specific heat anomaly.

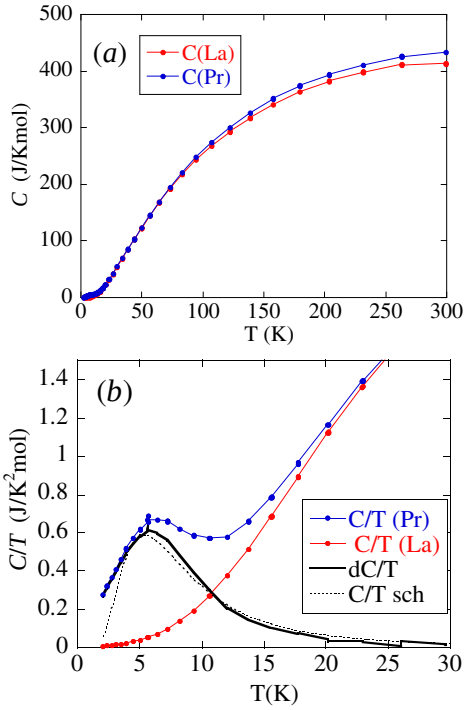

Figure 3. (a)Specific heats of the parent Ba_2PrBiO_6 and its related Ba_2LaBiO_6 compounds, C(Pr) and C(La). (b) Low temperature specific heats of both samples, C/T(Pr) and C/T(La). Specific heat differences dC/T in both compounds are also plotted. Dashed curves represent the calculated Schottky heat anomaly with $\triangle E$ =1.5 meV.

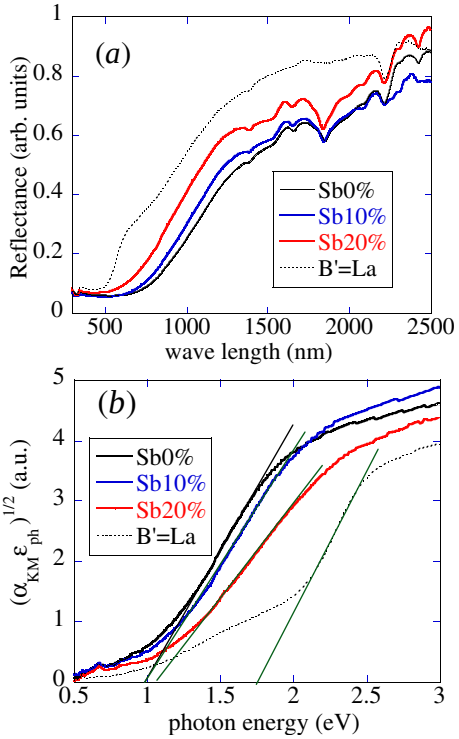

Figure 4. Optical measurements on $Ba_2Pr(Bi_{1-x},Sb_x)O_6$ (x=0, 0.1 and 0.2) powder samples. (a)Diffuse reflectance spectra as a function of wave length (b) Kubelka-Munk conversion of diffuse reflectance spectra as a function of photon energy. For the x=0 and x=0.2 samples, we evaluate $E_g = 0.977 \pm 0.023$ eV and 1.073 ± 0.014 eV, respectively. Straight lines denote the extrapolations to estimate the band gaps using the least squares method. For comparison, we exhibit the optical data of the Ba_2LaBiO_6 compound, giving $E_g = 1.767 \pm 0.028$ eV.

For $Ba_2Pr(Bi_{1-x},Sb_x)O_6$ (x=0, 0.1 and 0.2) powder samples, the diffuse reflectance spectra are shown in Fig.4 (a) as a function of wave length. First, the observed reflectance data for the powder samples are transformed to the absorption coefficient α_{KM} by using the conventional Kubelka-Munk function. Figure 4 (b) shows the square root of the absorption coefficient $(\alpha_{KM}\varepsilon_p)^{1/2}$ as a function of photon energy ε_p. For the Kubelka-Munk conversion data near the band edge, we extrapolate the tangent line to the ε_p axis and evaluate the optical band gaps from the intersection according to the equation of

$$(\alpha_{KM}\varepsilon_p)^{1/2} \propto (\varepsilon_p - E_g)$$

, where α_{KM}, ε_p, and E_g are the absorption coefficient, photon energy, and band gap [4, 5]. We estimate the values of band gaps to be $E_g = 0.977 \pm 0.023$ eV at $x = 0$, 1.003 ± 0.025 eV at $x = 0.1$ and 1.073 ± 0.014 eV at $x = 0.2$. For comparison, we also exhibit the optical data of the Ba_2LaBiO_6 compound, resulting in $E_g = 1.767 \pm 0.028$ eV. All band gaps are evaluated within errors of plus or minus several percent.

The effect of the band gap opening by the atomic substitution is supported by our first-principles electric structure calculation. We have calculated the band structure of Ba_2PrBiO_6 by using the density functional theory as implemented in the code VASP. The estimated band gap energy of the parent Ba_2PrBiO_6 is around 0.5 eV as shown in Fig5 (a) , leading to an underestimation in comparison to the experimental value. However, the band gap of Ba_2PrSbO_6 becomes 4.1 eV when we substitute Sb for Bi (Fig5 (b)). In addition, we obtain E_g=2.5 eV for the Ba_2LaBiO_6 where $B^{'}$ site is replaced by La (not shown here). These results probably predict the qualitative trends than the absolute values. The detailed analysis will be published elsewhere.

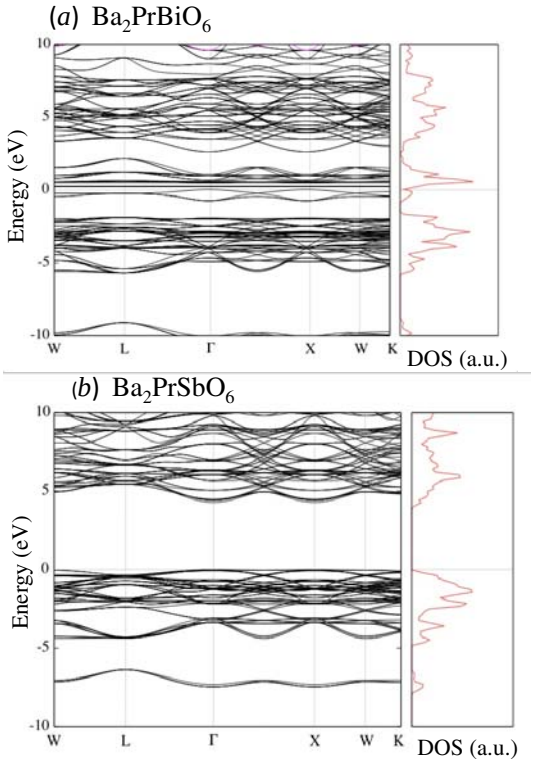

Figure 5. Energy band structures and total density of states (DOS) calculated by the density functional theory for (a) Ba_2PrBiO_6 and (b) Ba_2PrSbO_6 compounds. The band gaps are estimated to to be ~ 0.5 eV and 4.1 eV, for the parent Ba_2PrBiO_6 and Sb substituted Ba_2PrSbO_6 compounds, respectively.

4. Summary

We demonstrated crystal structures, magnetic, thermodynamic and optical properties of the B-site substituted perovskite oxides $Ba_2Pr(Bi_{1-x},Sb_x)\ O_6$ (x=0, 0.1 and 0.2). X-ray diffraction data point to the B-site ordered double-perovskite structure, which is consist with previous predictions based on the charge and ionic size differences. The magnetization and X-ray photoemission spectroscopy measurements considerably indicate the existence of Pr^{3+}, but do not exclude the presence of Pr^{4+}. The low temperature specific heat of the parent compound is well described by the Schottky heat anomaly due to crystal field splitting of Pr ion with $\triangle E$ =1.5 meV. The values of the band gap are evaluated to be 0.977$\pm$0.023 eV and 1.073$\pm$0.014 eV at the parent and Sb20% substituted samples, by using the conventional Kubelka-Munk function. The effect of band gap opening due to Sb substitution was examined by using the density functional theory.

5. Acknowledgment

The authors are grateful for Dr. K. Nonaka for his assistance in our experiments.

6. References

[1] Kobayashi K -I, Kimura T, Sawada H, Terakura K and Tokura Y, 1998 *Nature* **395** 677
[2] Ramesh R and Spaldin N A 2007 *Nature Materials* **6** 21
[3] Eng H W, Barnes P W, Auer B M and Woodward P M 2003 *J. Solid State Chem.* **175** 94
[4] Hatakeyama T, Takeda S, Ishikawa F, Ohmura A, Nakayama A, Yamada Y, Matsushita A and Yea J 2010 *J. Cer. Soc. Jpn.* **118** 91
[5] Matsushita A, Nakane T, Naka T, Isago H, Yamada Y and Yamada Yuh 2012 *Jpn. J. Appl. Phys.* **51** 121802
[6] Harrison W T A, Reis K P, Jacobson A J, Schneemeyer L F and Waszczak J V 1995 *Chem. Mater.* **7** 2161
[7] Vasala S and Karppinen M 2015 *Prog. Solid State Chem.* **43** 1
[8] Shannon R 1976 *Acta. Crystallogr.* **A32** 751
[9] Tang J W, Zou Z G and Ye J H 2007 *J. Phys. Chem.* **C111** 12779
[10] Kittel C 1976 *Introduction to Solid State Physics* sixth edition (New York: Wiley)